*ISET Journal of Earthquake Technology, Paper No. 609, Vol. 63, No. 2, June 2026, pp. 53-67*

# ESTIMATION OF DUCTILITY DEMAND FROM LINEAR RESPONSE PEAKS IN SINGLE-DEGREE-OF-FREEDOM SYSTEMS

Satya Kiran Raju Alluri
Department of Civil Engineering, Indian Institute of Technology Kanpur
Kanpur 208016, E mail id: *rajusk@nccr.gov.in*

Vinay K. Gupta*
Department of Civil Engineering, Indian Institute of Technology Kanpur
Kanpur 208016, E mail id: *vinaykg@iitk.ac.in*

Samit Ray Chaudhuri
Department of Civil Engineering, Indian Institute of Technology Kanpur
Kanpur 208016, E mail id: *samitrc@iitk.ac.in*

Ayan Sadhu
Department of Civil Engineering, Indian Institute of Technology Kanpur
Kanpur 208016, E mail id: *asadhu@uwo.ca*

## ABSTRACT

In performance-based seismic design, a structure is designed to attain multiple damage levels at different seismic hazard levels, and hence it is important to estimate structural damage, such as cracks in concrete beams and columns, for a hazard level, which is usually specified in the form of elastic response spectra. Structural damage can be quantified through the estimation and use of ductility and hysteretic energy demands consistent with the given response spectrum in an expression of damage index. It is convenient to estimate the two damage parameters directly from the response spectrum. This study considers such an estimation of ductility demand in the case of five different hysteretic models, i.e., elastic-perfectly-plastic, strain-hardening, stiffness-degrading bilinear, stiffness-degrading Riddell-Newmark, and pinching oscillators. Existing methods based on equivalent linearization technique and inelastic displacement ratio estimate maximum displacement by using the largest peak in the elastic displacement response. This study considers an alternative methodology based on the correlation of ductility demand with few largest peaks in the elastic response. A functional of those ordered peaks that exceed the yield level is considered and it is found that this functional has maximum correlation with ductility demand when only the largest peak is considered. This functional is then related to ductility demand via a single-parameter model, where the parameter is governed by the damping, period, hysteresis type, and maximum ductility demand of the oscillator. An exponential form is proposed for the variation of the model parameter with oscillator period for specific values of damping, maximum ductility demand, and hysteretic parameters. It is shown that except for stiff oscillators in certain period ranges, the proposed model works reasonably well. Further, for lower/higher damping ratios, the acceptable range of periods may decrease/increase and the model parameter versus oscillator period curves may be significantly different.

**KEYWORDS:** Performance-Based Seismic Design; Ductility Demand; Yield Displacement Level; Linear Excursions; Displacement Response Spectrum; Hysteretic Models

## INTRODUCTION

In the current seismic design practice, a structure is allowed to go into its nonlinear range of response when subjected to a strong earthquake shaking. This results in significant damage to the structure due to the repeated excursions of the response beyond its yield level. In order to ensure a desired performance of the structure, two important performance criteria are envisioned in the framework of performance-based seismic design (SEAOC, 1995). First, the structure should not collapse under the most severe earthquake motion anticipated at the site of the structure (i.e., for the maximum credible or safe shutdown earthquake). Second, the structure should not suffer excessive damage and should remain usable under a

https://doi.org/10.63898/ZWAN9633
*Corresponding Author

ground motion with higher probability of occurrence, say five times, than that for the most severe motion (i.e., for the design basis or operating basis earthquake). Thus, it is important to estimate the degree of structural damage under a given level of ground shaking, which is commonly characterized via a ground response spectrum.

Seismically induced structural damage, such as cracks in concrete beams and columns, can be correlated reasonably well with a quantitative measure termed as damage index using two important damage parameters: (i) ductility demand, and (ii) hysteretic energy demand (Park and Ang, 1985). Damage index is usually computed on the scale of one, with the zero value representing no damage and the value of one representing the collapse of the structure. The estimation of damage parameters, i.e., ductility demand and hysteretic energy demand, usually requires a nonlinear time-history analysis, which is time-consuming and often unnecessary from a design point of view. Thus, it becomes desirable to estimate damage parameters directly from the specified (elastic) response spectrum. This study considers the estimation of ductility demand, which is similar to estimating the maximum (nonlinear) displacement for a given yield displacement level.

Indirect methods have been proposed to estimate the maximum displacement of a nonlinear single-degree-of-freedom (SDOF) oscillator for a given seismic hazard (in the form of elastic response spectra) without resorting to the direct procedure of nonlinear time-history analyses. These include the use of equivalent linearization technique (ATC, 1995) and the use of inelastic displacement ratio (FEMA, 2000). Rosenblueth and Herrera (1964), Gulkan and Sozen (1974), Iwan (1980), etc. proposed formulations for the viscous damping and stiffness of an equivalent linear oscillator for direct use with the elastic spectrum. Several researchers have considered the use of inelastic displacement ratio $C$, which is multiplied with the maximum elastic displacement of the oscillator to estimate the maximum (nonlinear) displacement. Veletsos and Newmark (1960) and Veletsos et al. (1965) considered elasto-plastic hysteretic oscillators subjected to simple pulse and three recorded ground motions. They observed that at long periods, maximum nonlinear deformation is same as the maximum elastic deformation (i.e., $C = 1$), thus leading to the 'equal-displacement rule'. Newmark and Hall (1969), Riddell and Newmark (1979), Miranda (1993), and Rahnama and Krawinkler (1993) proposed periods above which the 'equal-displacement rule' could be applied. Ruiz-Garcia and Miranda (2003), Baez and Miranda (2000), and Miranda (2000) proposed $C_{\mu}(T)$ spectra describing the variations of $C$ with (initial) oscillator period for different levels of ductility demand $\mu$. These studies are particularly useful for the design of new structures when, for the type of structure being designed, an estimate of ductility supply is already available.

Inelastic displacement ratio spectra have also been studied and proposed for the evaluation of existing buildings (with known yield strength levels). These spectra, referred to as $C_R(T)$ spectra, describe the variations of $C$ with oscillator period for different levels of response reduction factor $R$. Shimazaki and Sozen (1984) considered five SDOF hysteretic models of varying strengths and two different periods with three recorded ground motions having different site periods and showed that $C$ varies significantly with $R$ only in the short-period region. Whittaker et al. (1998) considered 20 horizontal components of 10 ground motions on stiff soils or soft rock sites and showed that the maximum nonlinear deformation exceeds the maximum elastic displacement for $R > 5$ or for period $T$ smaller than about 1 s. Thus, the 'equal-displacement rule' is not applicable in these cases. Chopra and Goel (1999, 2000), Fajfar (1999, 2000) used $R$-$\mu$-$T$ relations to determine the $C_R(T)$ spectra. Miranda (2001) showed that this indirect approach leads to an underestimation of the maximum nonlinear displacement, and Ruiz-Garcia and Miranda (2003) proposed a model for the $C_R(T)$ spectra by carrying out nonlinear regression analyses on elasto-plastic oscillators using a suite of 216 accelerograms. Banerjee and Gupta (2022) and Dadheech and Gupta (2024) proposed models for the estimation of $C_R(T)$ spectra directly from the normalized relative velocity spectrum and normalized relative displacement spectrum, respectively, of the anticipated ground motion. These studies also provide a more detailed account of the past work based on the concept of inelastic displacement ratio.

The above studies have assumed the maximum inelastic displacement not to be governed by higher order peaks (i.e., second largest, third largest, … peaks) in the elastic displacement response. Even though the elastic response peaks do not have any obvious relationship with the inelastic response, the amplitudes and number of these peaks above the yield level measure the extent of the effort by the excitation that goes into damaging the structure. For example, if there are no peaks above the yield level, there is no such effort and no damage would result. If the 'linear excursions' beyond the yield level are stronger, the effort to cause the damage would be bigger resulting in greater damage in the system. Thus, it may be expected that a suitable functional of these 'linear excursions' would correlate well with a given damage parameter. Ductility demand is a commonly used damage parameter, particularly in the case of systems with little ductility supply, and therefore, efforts can be made to predict the ductility demand of a SDOF system by using the knowledge of linear excursions beyond the yield displacement level.

Based on the theses of the first and last authors (Sadhu, 2007; Alluri, 2010), this study looks at the possibility of estimating ductility demand in a SDOF oscillator, with a specified yield displacement level, from the knowledge of ordered peaks in its linear displacement response. A new functional, fictitious cumulative damage, of the linear excursions beyond the specified yield level is considered. A single-parameter model is also proposed to estimate ductility demand from this functional. This functional is then optimized over the number of largest excursions of the yield level, such that its correlation with the ductility demand is maximized. The parameter of the proposed model is estimated via linear regression analyses for the oscillators of 15 different periods and five different hysteretic models representative of different types of constructions and materials. Each regression analysis is done on the response of oscillators of six different yield strengths to a suite of 225 carefully selected ground motion records. The variation of the parameter of the proposed model with oscillator period is also modelled through exponential functions for the five types of oscillators with specific values of damping ratio, maximum ductility demand, and hysteretic parameter. The sensitivity of the results obtained to the possible variations in these parameters is also studied.

## PROPOSED MODEL

Damage in an oscillator is caused due to the excursions of (nonlinear) response beyond the yield displacement level, and it is expected that this would be correlated with the excursions by the linear response beyond the yield displacement level. Considering that ductility demand is the most popular damage parameter, where ductility demand of a nonlinear system is the ratio of maximum displacement response of the system during the excitation to its yield displacement level, this study considers the correlation of ductility demand with the extent to which linear displacement peaks cross the yield displacement level. To this end, we consider a simple 'Fictitious Cumulative Damage' functional that is based on the averaging of the amplitudes of the excursion peaks relative to the yield level, without considering the order of excursions:

$$\mathrm{FCD} = \frac{1}{N_e}\sum_{i=1}^{N_e}\frac{X_i}{X_y} \tag{1}$$

Here, $X_i$ $(\geq X_y)$ is the *i*th largest peak amplitude in the absolute linear displacement response $|X(t)|$ of the oscillator exceeding the specified yield displacement level $X_y$, and $N_e$ is the total number of excursions by the (absolute) linear displacement response. It may be noted that $X_1 \geq X_2 \geq \ldots \geq X_{N_e} \geq X_y$, and $X_y > X_{N_e+1} \geq X_{N_e+2} \geq \ldots$. Figures 1(a) and 1(b) illustrate various terms used in Equation (1) with the help of linear response time-history and force-displacement curve, respectively, in the case of $N_e = 5$ and elastic-perfectly-plastic (EPP) oscillator.

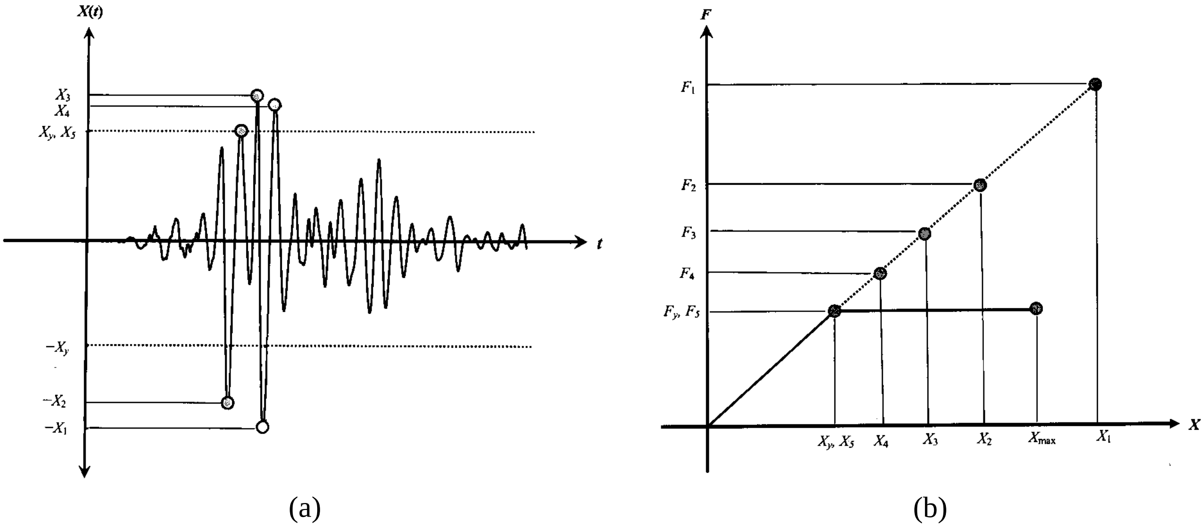


Fig. 1 Excursion Peaks in the (a) Linear Displacement Response and (b) Force-Displacement Relationship of the EPP Oscillator in Case of $N_e = 5$

The proposed functional is assumed to be related to ductility demand $\mu$ as

$$\mu = (\mathrm{FCD})^P \tag{2}$$

where *P* is a parameter governed by the initial period and type of nonlinear oscillator. Before proceeding further, it will be desirable to check the extent of correlation between FCD and $\mu$. It is expected that this correlation will be very poor for stiff oscillators. For such oscillators, irrespective of the level of ductility demand, the values of $X_1$ and $X_y$ will be very close and therefore, FCD will approach unity as the period goes to zero. It will be therefore useful to know the shortest period above which such good correlation, if it is indeed there, can be assumed to exist. A suite of 225 accelerograms considered by Sen and Gupta (2018) and 30 EPP oscillators with five different periods and six different yield levels are considered to check the extent of linear correlation between $\ln \mu$ and $\ln \mathrm{FCD}$.

The 225 accelerograms considered in the suite have been recorded during 36 earthquake events in western U.S.A between 1954 and 1984 (see Lee and Trifunac (1987) for details) and during the 1994 Northridge earthquake. All records have peak ground accelerations (PGAs) from 0.04*g* to 0.83*g*, and have (published) magnitudes $M$ ranging from 3.2 to 6.7, epicentral distances up to 223 km, and site conditions from alluvium to rock. The S40E component of the motion recorded at the El Centro Array-4 site during the 1994 Northridge earthquake is considered as the reference ground motion, and all the 225 ground motions are scaled up/down to the peak ground acceleration (= 0.48*g*) of the reference ground motion. Figure 2 shows the 'Mean − SD', 'Mean', and 'Mean + SD' levels of the Fourier spectra of the scaled ground motions, where SD refers to the standard deviation and these levels are computed at any period on the logarithmic scale. It is clear from the 'almost uniform' distribution of Fourier amplitudes across different periods for any of these levels that the ground motions considered here cover a wide range in terms of frequency content.

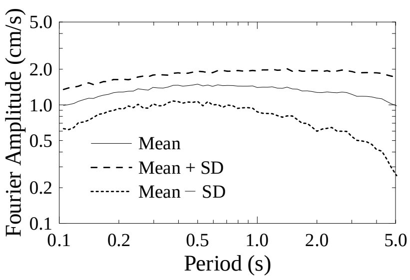


Fig. 2 Mean, Mean+SD, and Mean–SD Levels of Fourier Spectra for the Suite of 225 Scaled Ground Motions

The oscillators considered have 15 periods: 0.1, 0.2, 0.3, 0.4, 0.5, 0.6, 0.7, 0.8, 0.9, 1.0, 1.2, 1.4, 1.6, 1.8, and 2.0 s. For a period, six equispaced values of yield strengths are considered such that the lowest and highest values of these correspond to the ductility demands of 1 and 8, respectively, in response to the reference ground motion. The initial damping is assumed to be 5% of the critical damping. The (nonlinear) time-history analyses for all 90 oscillators are performed numerically by using the Newmark-$\beta$ method with $\beta$ = 1/4 and $\gamma$ = 1/2 (corresponding to the average acceleration method) and step size as ! $t = 0.002$ s.

For a given period, ductility demand $\mu$ and functional FCD are computed for each of the ($6 \times 225$ =) 1350 combinations of ground motions and yield strengths. Further, correlation coefficients are computed between ln $\mu$ and ln FCD, while ignoring those combinations for which $\mu$ < 1 and $\mu$ > $\mu_{\max}$, with $\mu_{\max}$ being varied from 1.5 to 8 at the interval of 0.5. Figure 3 shows the variation of correlation coefficient with $\mu_{\max}$ for the oscillators with 0.2, 0.5, 0.9, 1.4 and 2.0 s periods. It is clear from the figure that the linear correlation between ln $\mu$ and ln FCD becomes poorer as $\mu_{\max}$ increases and/or as the oscillator period decreases. Also, there is an asymptotic value for an oscillator with period $\geq$ 0.5 s which correlation coefficient tends to reach at higher $\mu_{\max}$. This asymptotic value is almost achieved at $\mu_{\max}$ = 8. Considering that a correlation coefficient of 0.8 or more may be reasonable for a proper "best straight-line fit" between the two variables, it can be concluded that $\mu$ is well-correlated with FCD for the EPP oscillators with periods > 0.3 s, irrespective of the ductility range, and for the stiffer oscillators in the case of ductility range of 1–3. Further, it is justified to consider the proposed functional FCD and to estimate the parameter *P* in Equation (2) for different periods of the EPP oscillator. It is assumed that Equation (2) will also work for the other types of nonlinear oscillators.

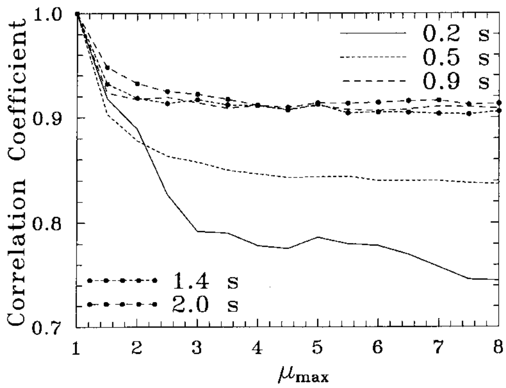


Fig. 3 Variation of Correlation Coefficient of ln FCD and ln $\mu$ with $\mu_{\max}$ for Different Oscillator Periods in Case of EPP Oscillator

While the definition of FCD in Equation (1) is based on all the peaks crossing the yield displacement level, it is possible that only a few large peaks correlate with the maximum nonlinear displacement. Indeed, for flexible oscillators, the maximum nonlinear displacement approaches the maximum linear displacement and thus correlates only with the largest peak in the linear response. Thus, an investigation is carried out in the cases of five types of nonlinear oscillators to study the correlation between ln FCD and ln $\mu$ as a function of the percentage of $N_e$ (linear) peaks beyond the yield displacement level which are used in place of $N_e$ for the computation of FCD in Equation (1).

The numerical analysis carried out above is repeated, specifically for the oscillators of 0.1, 0.4, 0.8, 1.4, and 2.0 s periods and $\mu_{\max}$ = 8, in the case of each of the five types of nonlinear oscillators. For the Newmark-$\beta$ method, step size is taken as ! $t$ = 0.001 s. With *k* denoting the initial stiffness and $X_y$ the yield displacement, the five types of nonlinear oscillators used here are as follows:

(a) Elastic-perfectly-plastic (EPP) oscillator, which is considered as a simple idealization of the ductile non-degrading structural systems, such as unbraced steel frames under moderate axial loads, and eccentrically braced frames. Figure 4(a) shows the hysteretic model for this oscillator.

(b) Strain-hardening (SH) oscillator, which is generally considered as an idealization of the steel structures. Figure 4(b) shows the hysteretic model for this oscillator, where $r$ is the strain-hardening ratio (i.e., the ratio of post-yielding to pre-yielding stiffness), taken as 0.03 in this study.

(c) Stiffness-degrading bilinear (SDB) oscillator (Nielsen and Imbeault, 1970), for which the hysteretic model is shown in Figure 4(c). This model is similar to the SH oscillator, except that the loading and unloading stiffnesses degrade with the previous maximum displacement. The unloading stiffness remains constant until the response displacement amplitude exceeds the previous maximum displacement in any direction. The degrading stiffness $k_u$ is defined as

$$k_u = k\left[\frac{X_y}{X_m}\right]^{\alpha} \tag{3}$$

where $\alpha$ is the unloading stiffness-degrading parameter, taken as 0.5 in this study; and $X_m$ is the previously attained maximum displacement in any direction. This model is sometimes considered as an idealization for the reinforced concrete members, frames, and walls. In this study, the strain-hardening ratio $r$ is taken as 0.03.

(d) Stiffness-degrading Riddell-Newmark (SDRN) oscillator (Riddell and Newmark, 1979), which is like the SDB oscillator and is often considered as an idealization for the reinforced concrete members, frames, and walls. Figure 4(d) shows the hysteretic model for this oscillator. This model consists of an initially bilinear spline, and loading occurs either on the strain-hardening branch or towards the farther point attained in the previous cycle. The unloading stiffness is same as the initial stiffness $k$. In this study, the strain-hardening ratio $r$ is taken as 0.03.

(e) Pinching oscillator, which is often utilized to model the wood-frame buildings and masonry-infilled concrete frames. This model is similar to a stiffness-degrading oscillator, except that this also accounts for some initial slip while the reloading takes place. Figure 4(e) shows the hysteretic model for this oscillator, where $r_1$ is the ratio of the stiffness during slip to that in the pre-yielding phase, and $r_2$ is the ratio of the stiffness during reloading to that in the pre-yielding phase. These ratios are functions of previous maximum displacements in the corresponding directions. There are several pinching models (from simple to very complex) that have been utilized in the previous studies. This study uses the 'pinching4' model of OpenSees (Mazzoni et al., 2007). The input parameters for this model are taken same as those obtained by Kanvinde and Deierlein (2006) for a wood-frame building and are listed in Table 1, with the strain-hardening ratio $r$ taken as 0.3.

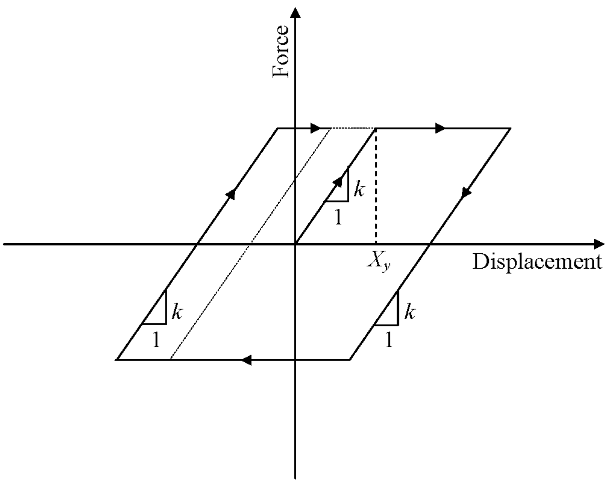


(a)

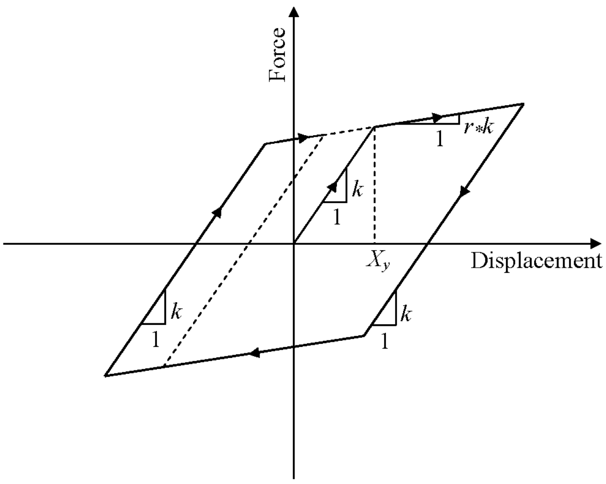


(b)

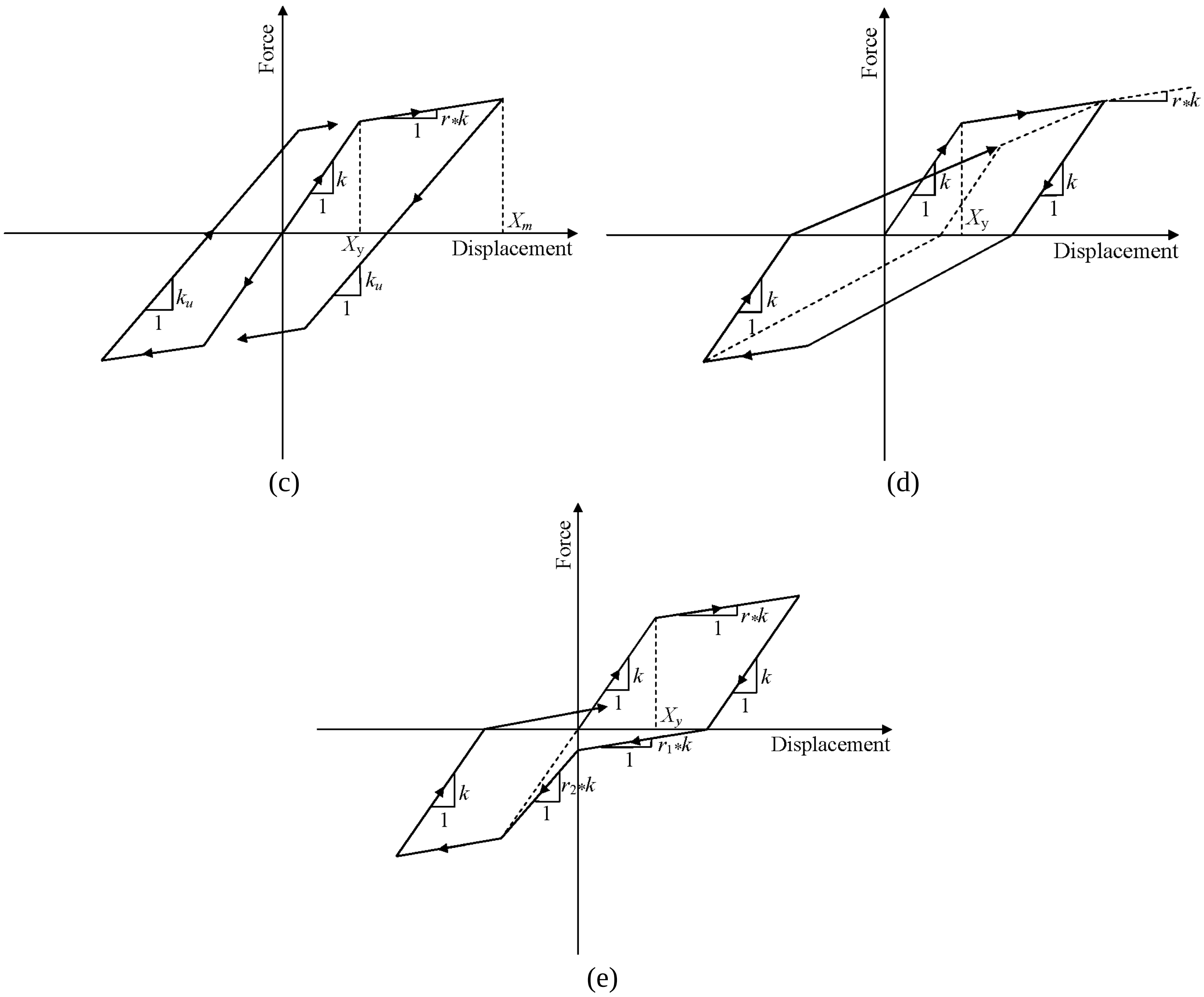


Fig. 4 Hysteretic Model for (a) EPP, (b) SH, (c) SDB, (d) SDRN, and (e) Pinching Oscillator

**Table 1: Values of input (OpenSees) parameters for pinching model**

| Parameter | Value | Parameter | Value | Parameter | Value |
|---|---|---|---|---|---|
| rDispP | 0.56 | gK2 | 1.20 | gD4 | 1.50 |
| rDispN | 0.56 | gK3 | 0.00 | gDLim | 0.50 |
| rForceP | 0.40 | gK4 | 0.30 | gF1 | 0.00 |
| rForceN | 0.40 | gKLim | 0.90 | gF2 | 1.80 |
| uForceP | 0.00 | gD1 | 0.00 | gF3 | 0.00 |
| uForceN | 0.00 | gD2 | 1.00 | gF4 | 1.20 |
| gK1 | 0.00 | gD3 | 0.00 | gFLim | 1.00 |

Figures 5(a)–5(e) show how the correlation between $\ln \mathrm{FCD}$ and $\ln \mu$ varies with the percentage of ordered peaks considered in FCD for the EPP, SH, SDB, SDRN, and pinching oscillators, respectively, of the five different periods. The zero value in each of these figures refers to only the largest peak (i.e., the spectral displacement) being considered in the calculation of FCD. It may be observed in these figures that correlation decreases as a greater number of ordered peaks are considered in the expression of FCD (see Equation (1)) in place of $N_e$ and that correlation is largest when only the largest peak is considered. These trends are observed irrespective of the type and period of nonlinear oscillator. Hence, the functional FCD is modified, by replacing $N_e$ by 1, to

$$F = \frac{X_1}{X_y} \tag{4}$$

such that

$$\mu = F^{P} \tag{5}$$

becomes the estimate of ductility demand.

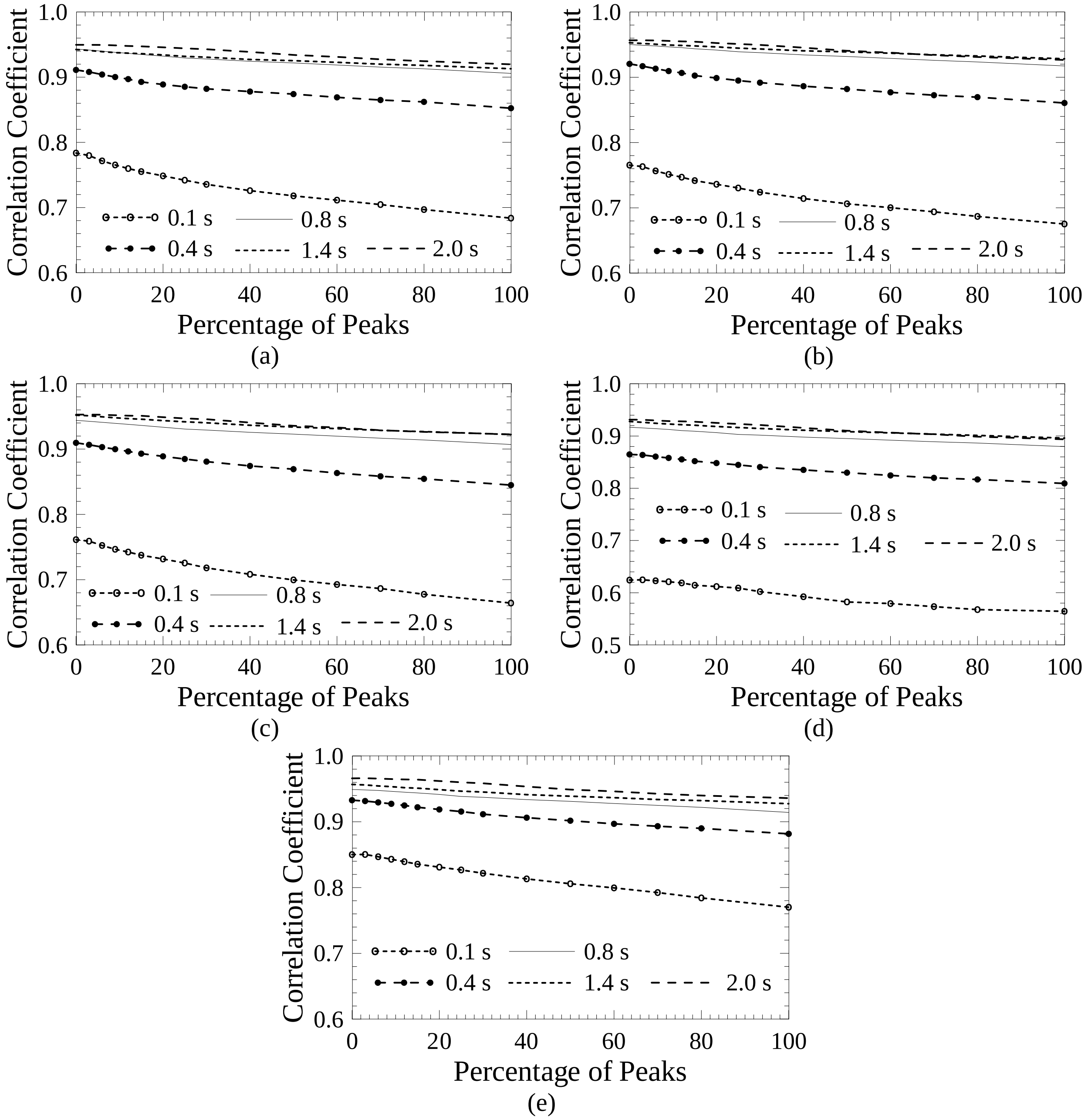


Fig. 5 Variations of Correlation Coefficient with Percentage of Peaks Considered in FCD in Case of (a) EPP Oscillator, (b) SH Oscillator, (c) SDB Oscillator, (d) SDRN Oscillator, and (e) Pinching Oscillator, for Different Oscillator Periods

## ESTIMATION OF PARAMETER *P*

Before the estimation of *P*, it is desirable to evaluate the performance of the proposed estimation of ductility demand according to Equations (4) and (5) for all the five types of oscillators at the period range of interest. Hence, the correlation analysis carried for Figure 5 is repeated between the actual values of ductility demand $\mu$ and functional $F$ for the same fifteen oscillators with different periods as considered for Figure 3. Figure 6 shows the variations of correlation coefficient between $\ln F$ and $\ln \mu$ with the period of oscillator for each of the five types of oscillators. It may be observed from this figure that the correlation coefficient between $\ln F$ and $\ln \mu$ increases with period and is not so good for the SDRN oscillators. Lower correlation observed for the stiff oscillators is consistent with the common knowledge that in the acceleration-sensitive zone the nonlinear response loses correlation with the linear response. Considering again that a correlation coefficient of 0.8 and above may be sufficient for an adequate linear correlation between $\ln F$ and $\ln \mu$, the proposed estimation of ductility demand is likely to perform reasonably well for the oscillators considered, other than the SDRN oscillator, with periods greater than 0.13 s. For a SDRN oscillator, the period of oscillator should not be less than 0.3 s.

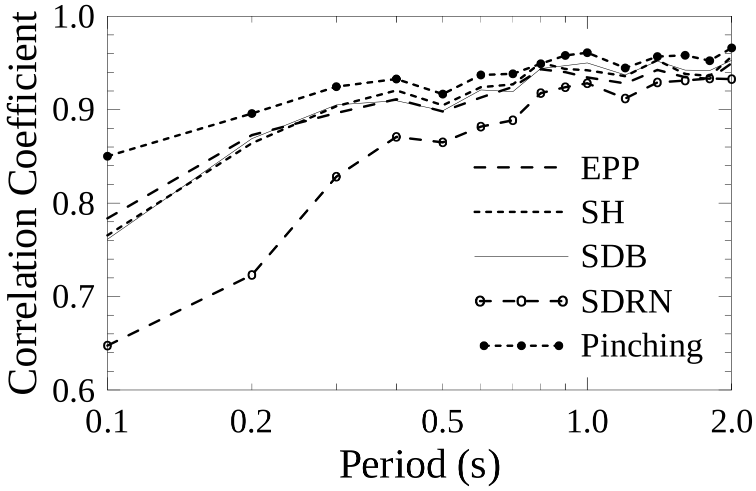


Fig. 6 Variations of Correlation Coefficient with Oscillator Period for Different Types of Oscillators

Linear regression analyses are carried out to estimate the best-fit values of the parameter *P* for all five types of oscillators at different periods, by using the same pairs of (actual) $\mu$ and *F* values as used above for finding the correlation coefficients shown in Figure 6. The periods considered are greater than 0.3 s for the SDRN oscillator and greater than 0.13 s for the remaining oscillators. Figures 7(a)–7(e) show the variations of (best-fit) *P* with period in the cases of EPP, SH, SDB, SDRN, and pinching oscillators, respectively. These figures also show the modelled variations in the form of the following curve:

$$P = aT^{-b} \tag{6}$$

where *T* represents the period of the oscillator, and *a* and *b* are the best-fit constants as given in Table 2 for different types of oscillators. It may be observed in each of the figures that *P* decreases with the period of the oscillator, which is consistent with the fact that *P* should decrease to unity as *T* goes to infinity. However, the proposed expression of *P* does not take this limiting behaviour into account and is meant to be applicable only for the periods (from 0.13 or 0.3 s, depending on the type of oscillator) up to 2.0 s. It may be difficult to find a single expression of *P*, both for the periods up to and beyond 2.0 s, because *P* can become less than unity for the intermediate periods (see Figures 7(a)–7(e)) and thus should increase with *T* for the periods longer than those periods. It may be also observed from a comparison of Figures 7(a)–7(e) that leaving the case of SH oscillator, the type of nonlinearity does not make significant difference to the value of *P* for the oscillators with periods longer than 0.7 s. Hence, a single universal expression of *P* may be feasible for a large variety of oscillators, in place of Equation (6) and Table 2, in this range.

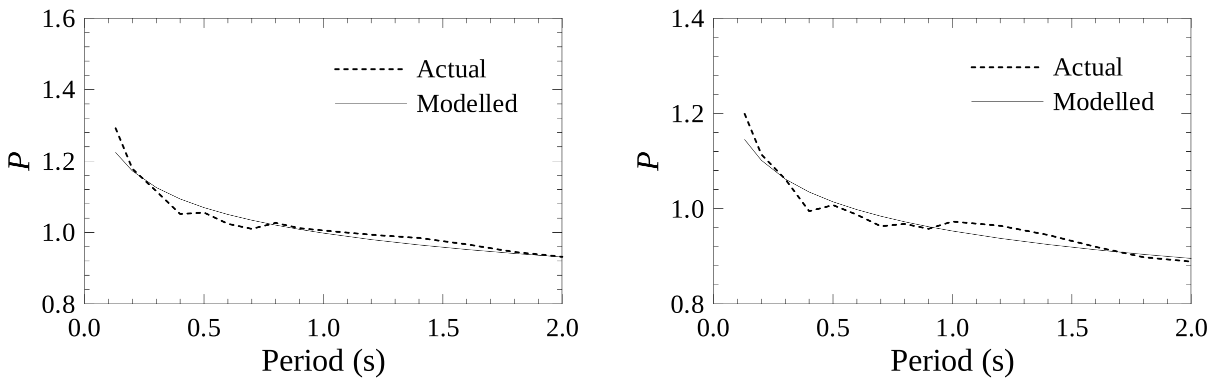


(a) (b)

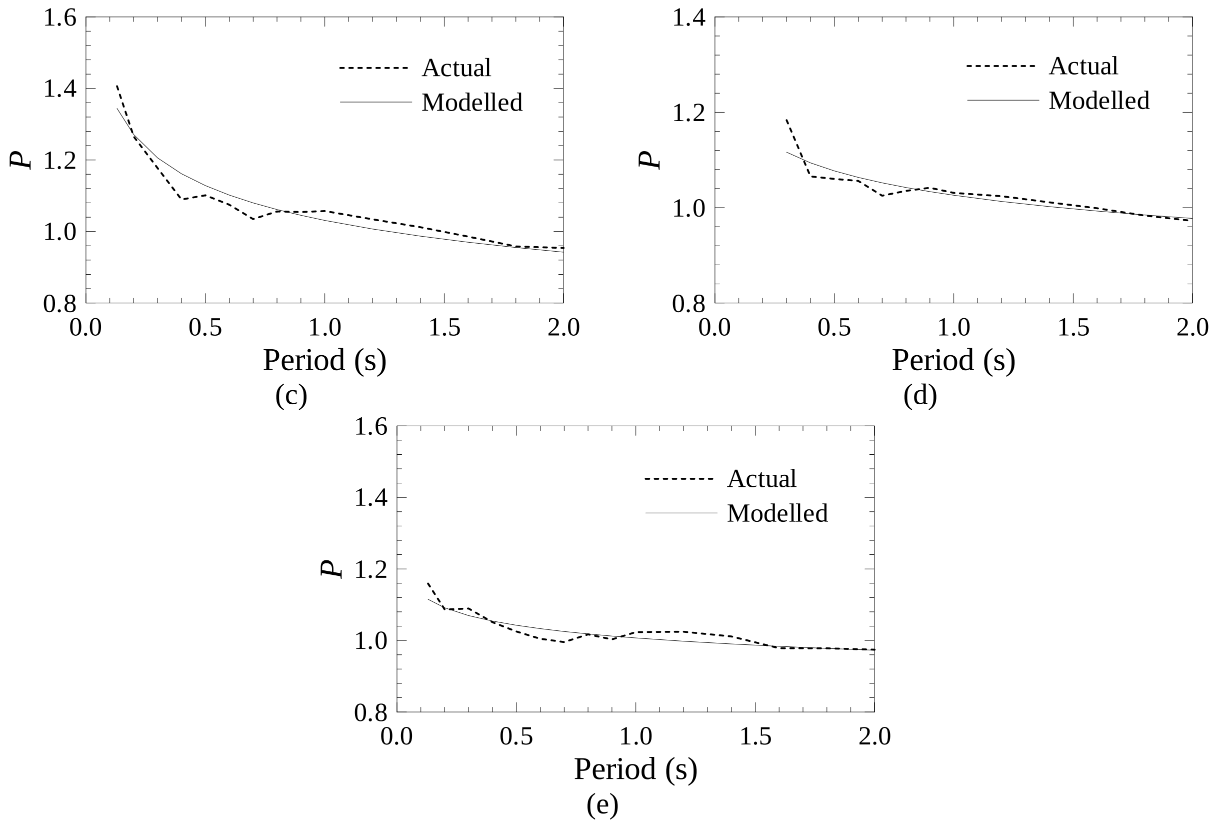


Fig. 7 Actual and Modelled Variations of Parameter $P$ with Oscillator Period for (a) EPP Oscillator, (b) SH Oscillator, (c) SDB Oscillator, (d) SDRN Oscillator, and (e) Pinching Oscillator

**Table 2: Best-fit values of constants *a* and *b* in Equation (6) for different types of oscillators**

| Type of Oscillator | $a$ | $b$ |
|---|---|---|
| **EPP** | 0.998 | 0.10 |
| **SH** | 0.953 | 0.09 |
| **SDB** | 1.031 | 0.12 |
| **SDRN** | 1.026 | 0.07 |
| **Pinching** | 1.007 | 0.05 |

The levels of uncertainty in the actual values of $P$ plotted in Figures 7(a)–7(e) are shown in Figure 8. This uncertainty is due to the modelling of ductility demand as in Equations (4) and (5) and due to the uncertain role of temporal features in the ground motion. Each curve in Figure 8 shows, at a period, the coefficient of variation (COV) obtained from the values of $P$ corresponding to the ‘best-fit’ and ‘best-fit plus one standard deviation’ estimates of $\ln\mu$. Here, the ‘best-fit’ estimates of $\ln\mu$ refer to the values obtained from Equation (5) on using the best-fit estimates of $P$. For the ‘best-fit plus one standard deviation’ estimates of $\ln\mu$, in the case of a given combination of period and oscillator type, the scatter diagram of $\ln\mu$ with $\ln F$ is considered and the values of standard deviation in $\ln\mu$ are calculated over 30 intervals of $\ln F$. These values are then added to the ‘best-fit’ estimates of $\ln\mu$. The value of $P$ giving best-fit to the so-obtained values of $\ln\mu$ is considered to represent the mean plus standard deviation level of $P$ as compared to the mean level for its best-fit estimate. It may be observed that the degree of uncertainty is almost same for different types of oscillators and almost invariant of the period of oscillator for the periods longer than 0.4 s. Except for very short periods, the COV values are less than 0.2, and for most periods those are around 0.1. Thus, the proposed model of ductility demand in terms of the normalized largest linear response peak can be considered as appropriate for the ‘not too stiff’ oscillators.

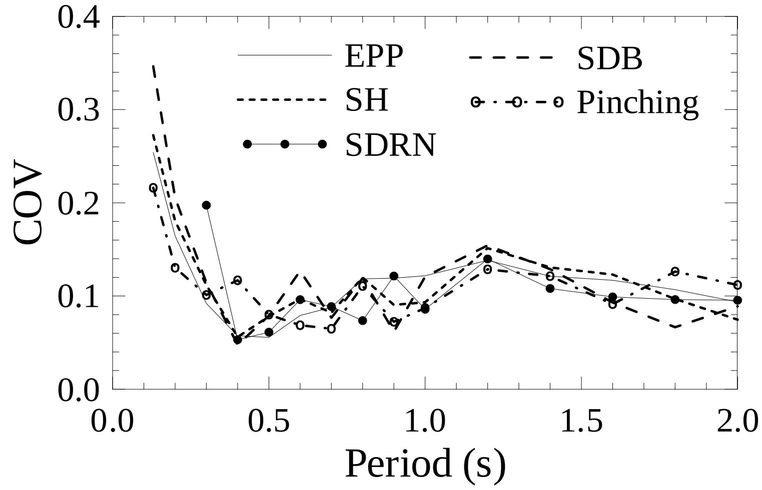


Fig. 8 Variations of COV in Actual $P$ with Oscillator Period for Different Types of Oscillators

## SENSITIVITY OF RESULTS

The results given above are for the 5%-damping oscillators with maximum ductility demand limited to the value of 8 and with specific values of the parameters for hysteretic behaviour. It will be interesting to also consider the oscillators with 2% and 10% damping, and with maximum ductility demand limited to the values of 4 and 6. It will also be desirable to consider the possible variations in the value of strain-hardening ratio $r$ in the case of the SDRN and pinching types of oscillators and unloading stiffness-degrading parameter $\alpha$ in the case of the SDB type of oscillators.

Figure 9 shows the comparison of the variations of correlation coefficient between $\ln F$ and $\ln \mu$ with the period of the EPP oscillator for the damping ratios equal to 2%, 5%, and 10%. It is clear from this figure that the proposed model of ductility demand works for stiffer oscillators (than those acceptable for the 5% damping ratio) in the case of greater damping, while a lower damping reduces the range of periods in which the proposed model can be considered acceptable. Similar results are observed for the SH, SDB, SDRN, and pinching types of oscillators, and thus the proposed model may not work so well for a lightly damped oscillator of given period due to the possible increase in its maximum inelastic excursion.

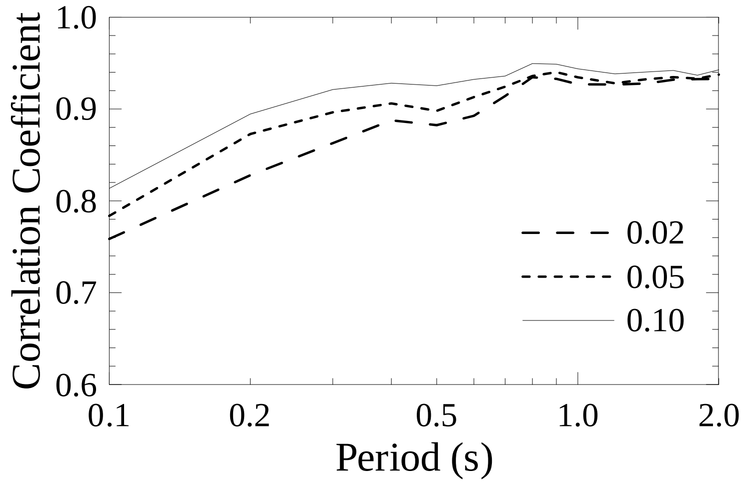


Fig. 9 Variations of Correlation Coefficient with Oscillator Period for Different Damping Ratios in the Case of EPP Oscillator

Figure 10 shows the comparison of the variations of correlation coefficient between $\ln F$ and $\ln \mu$ with the period of the SH oscillator for the maximum ductility demand limited to the values of 4, 6, and 8. It may be observed that at the intermediate to long periods, correlation coefficient remains undisturbed if the maximum ductility demand is limited to a value lower than 8. There is however a minor improvement in the correlation coefficient at short periods. This trend is observed in the EPP, SDB, SDRN, and pinching types of oscillators also, and hence the proposed model may be considered to work on slightly stiffer oscillators also, when there is a possibility of reduced maximum inelastic excursion due to the reduced maximum ductility demand.

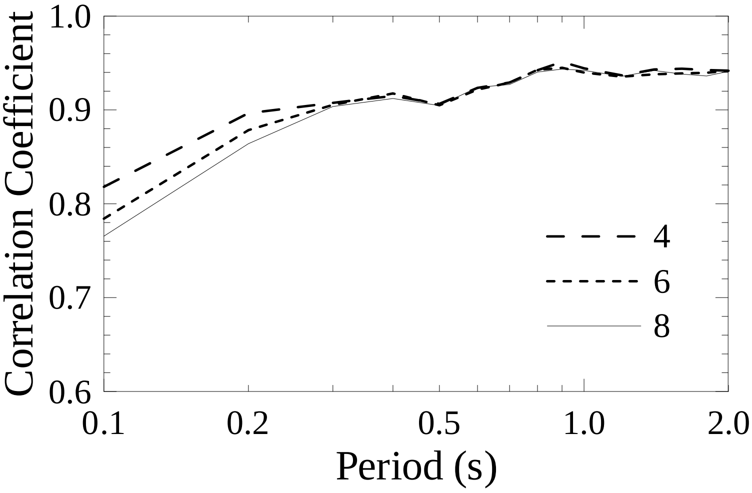


Fig. 10 Variations of Correlation Coefficient with Oscillator Period for Different Maximum Ductility Demands in the Case of SH Oscillator

The correlation coefficient between $\ln F$ and $\ln \mu$ is also recalculated when $\alpha$ in the case of the SDB type of oscillators becomes equal to 0.25 and 0.75 (instead of 0.50), and $r$ in the cases of the SDRN and pinching types of oscillators becomes equal to 0.06, 0.10, and 0.15 (instead of 0.03) and to 0.20 and 0.25 (instead of 0.30), respectively. It is seen that the correlation coefficient changes little with the change in these parameters at any period. For example, Figure 11 shows the comparison of the variations of correlation coefficient with the period of the pinching oscillator for the strain-hardening ratios equal to 0.20, 0.25, and 0.30. It may therefore be assumed that the proposed model is applicable (or not applicable) to a particular type of oscillator irrespective of the value of its hysteretic behaviour parameter.

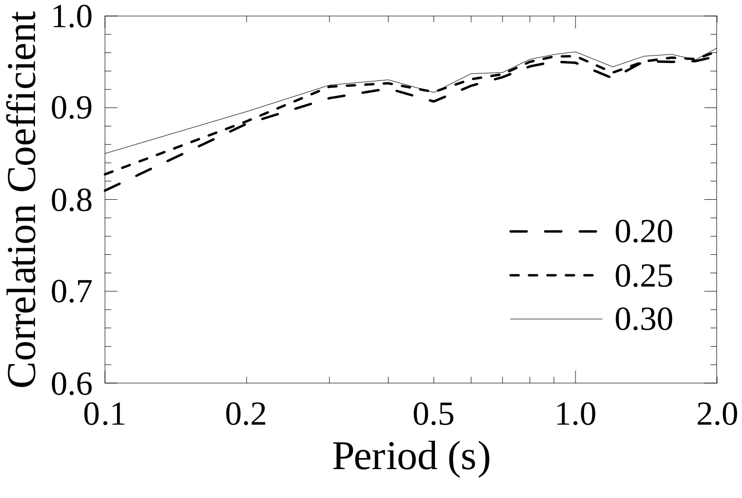


Fig. 11 Variations of Correlation Coefficient with Oscillator Period for Different Strain-Hardening Ratios in the Case of Pinching Oscillator

Figures 12(a)–12(c) show the variations in the best-fit values of $P$ with oscillator period $T$ for the cases considered in Figures 9–11, respectively. Only those periods are considered in these figures for which the correlation coefficient is at least equal to 0.8. It may be observed that irrespective of the extent to which correlation coefficient is sensitive to the variations in damping ratio, maximum ductility demand, and hysteretic behaviour parameter, the $P$ versus $T$ curves may become significantly different (from those given in Figures 7(a)–7(e)) with these variations, particularly in the case of different damping ratios.

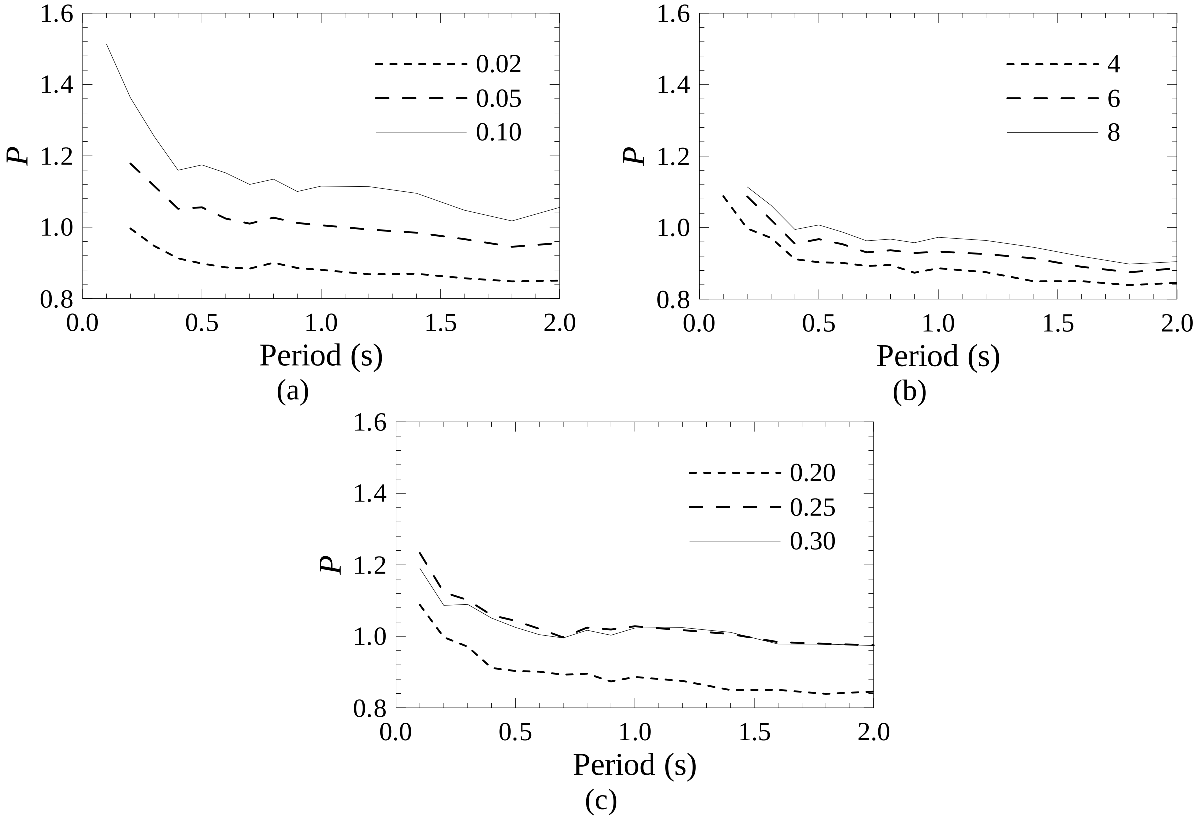


Fig. 12 Variations in Actual $P$ with Oscillator Period for Different (a) Damping Ratios in the Case of EPP Oscillator, (b) Maximum Ductility Demands in the Case of SH Oscillator, (c) Strain-Hardening Ratios in the Case of Pinching Oscillator

## SUMMARY AND CONCLUSIONS

A single-parameter model has been developed to estimate ductility demand of a SDOF oscillator using the linear displacement response peaks to the anticipated ground motion in the cases of elastic-perfectly-plastic (EPP), strain-hardening (SH), stiffness-degrading bilinear (SDB), stiffness-degrading Riddell-Newmark (SDRN), and pinching oscillators. This model uses a 'Fictitious Cumulative Damage' functional (FCD) of the linear excursions (i.e., the linear peaks greater than the specified yield displacement) and involves a parameter $P$ to be obtained from a linear regression analysis. On considering an optimum number of such excursions, it has been found that consideration of only the largest peak, which is available from the displacement response spectrum of the anticipated ground motion, gives the best correlation of FCD with ductility demand.

On considering a suite of 225 ground motions and six levels of yield strengths, it has been found that the proposed model can be reliably used for the oscillator periods greater than 0.13 s in the case of EPP, SH, SDB, and pinching oscillators and 0.3 s in the case of SDRN oscillator. For the acceptable ranges of periods, exponential forms describing the variations of the parameter $P$ with oscillator period have been proposed for the five types of oscillators in the case of 5% damping, maximum ductility demand of 8, and for specific values of the hysteresis parameters. It has also been observed that for lower/higher damping ratios, the acceptable range of periods may decrease/increase and that the model parameter versus oscillator period curves may also be significantly different.

The proposed model of ductility demand, together with the exponential form of the parameter $P$ of this model, has been illustrated by Alluri (2010) by calculating damage in the case of two concrete bridges idealized as SDOF systems. The proposed approach of using linear peaks can also be used for the estimation of hysteretic energy demand in SDOF oscillators by considering only the 25% largest linear excursions (Sen and Gupta, 2018). Sen and Gupta (2018) have also shown how this approach can be used to quantify structural damage in the case of 2-DOF and 3-DOF shear frames.

It may be mentioned that for the five types of hysteretic oscillators considered in this study, the proposed model of ductility demand is similar to the concept of inelastic displacement ratio, considering that both effectively use elastic spectral displacement to estimate the peak inelastic deformation. Further, this study has not discussed the confidence levels associated with the ductility demand values predicted by the proposed model. Hence, a comprehensive study needs to be carried out to determine the relative performance of the proposed model vis-à-vis the existing models of inelastic displacement ratio in terms of the errors associated with their predictions. Such a study may also consider a wider range of pinching oscillators (than that implied by the model parameters in Table 1) and periods longer than 2 s.

## REFERENCES

1. Alluri, S.K.R. (2010). "On Estimation of Seismic Damage from Linear Response Peaks", *M.Tech. Thesis, Indian Institute of Technology Kanpur, Kanpur*.
2. ATC (1995). "Structural Response Modification Factors", *Report ATC-19, Applied Technology Council, Redwood City, U.S.A.*
3. Baez, J.I. and Miranda, E. (2000). "Amplification Factors to Estimate Inelastic Displacement Demands for the Design of Structures in the Near Field", *Proceedings of the Twelfth World Conference on Earthquake Engineering, Auckland, New Zealand*, Paper No. 1561 (on CD).
4. Banerjee, A. and Gupta, V.K. (2022). "A Statistical Study of Inelastic Displacement Ratio Spectrum for Existing Structures", *Earthquake Engineering and Resilience*, Vol. 1, No. 4, pp. 454–479.
5. Chopra, A.K. and Goel, R.K. (1999). "Capacity-Demand-Diagram Methods Based on Inelastic Design Spectrum", *Earthquake Spectra*, Vol. 15, No. 4, pp. 637–656.
6. Chopra, A.K. and Goel, R.K. (2000). "Evaluation of a NSP to Estimate Seismic Deformation: SDF Systems", *Journal of Structural Engineering, ASCE*, Vol. 126, No. 4, pp. 482–490.
7. Dadheech, S. and Gupta, V.K. (2024). "Estimation of Inelastic Displacement Ratio Spectrum for Existing RC Structures via Displacement Response Spectrum", *Earthquake Engineering & Structural Dynamics*, Vol. 53, No. 15, pp. 4806–4829.
8. Fajfar, P. (1999). "Capacity Spectrum Method Based on Inelastic Demand Spectra", *Earthquake Engineering & Structural Dynamics*, Vol. 28, No. 9, pp. 979–993.
9. Fajfar, P. (2000). "A Nonlinear Analysis Method for Performance-Based Seismic Design", *Earthquake Spectra*, Vol. 16, No. 3, pp. 573–592.
10. FEMA (2000). "Prestandard and Commentary for the Seismic Rehabilitation of Buildings", *Report FEMA-356, Federal Emergency Management Agency, Washington, DC, U.S.A.*
11. Gulkan, P. and Sozen, M. (1974). "Inelastic Response of Reinforced Concrete Structures to Earthquake Motions, *ACI Structural Journal*, Vol. 71, No. 12, pp. 604–610.
12. Iwan, W.D. (1980). "Estimating Inelastic Response from Elastic Response", *Earthquake Engineering & Structural Dynamics*, Vol. 8, No. 4, pp. 375–388.
13. Kanvinde, A.M. and Deierlein, G.G. (2006). "Analytical Models for the Seismic Performance of Gypsum Drywall Partitions", *Earthquake Spectra*, Vol. 22, No. 2, pp. 391–411.
14. Lee, V.W. and Trifunac, M.D. (1987). "Strong Earthquake Ground Motion Data in EQUINFOS: Part I", *Report No. CE 87-01, University of Southern California, Los Angeles, U.S.A.*
15. Mazzoni, S., McKenna, F., Scott, M.H. and Fenves, G.L. (2007). "OpenSees Command Language Manual", *Technical Report, Pacific Earthquake Engineering Research Center, University of California, Berkeley, U.S.A.*
16. Miranda, E. (1993). "Evaluation of Site-Dependent Inelastic Seismic Design Spectra", *Journal of Structural Engineering, ASCE*, Vol. 119, No. 5, pp. 1319–1338.
17. Miranda, E. (2000). "Inelastic Displacement Ratios for Structures on Firm Sites", *Journal of Structural Engineering, ASCE*, Vol. 126, No. 10, pp. 1150–1159.
18. Miranda, E. (2001). "Estimation of Inelastic Deformation Demands of SDOF Systems", *Journal of Structural Engineering, ASCE*, Vol. 127, No. 9, pp. 1005–1012.

19. Newmark, N.M. and Hall, W.J. (1969). "Seismic Design Criteria for Nuclear Reactor Facilities", *Proceedings of the Fourth World Conference on Earthquake Engineering, Santiago, Chile*, Vol. II, No. B-4, pp. 37–50.
20. Nielsen, N.N. and Imbeault, F.A. (1970). "Validity of Various Hysteretic Systems", *Proceedings of the Third Japan Earthquake Engineering Symposium, Tokyo, Japan*, pp. 707–714.
21. Park, Y.J. and Ang, A.H.-S. (1985). "Mechanistic Seismic Damage Model for Reinforced Concrete", *Journal of Structural Engineering, ASCE*, Vol. 111, No. 4, pp. 722–739.
22. Rahnama, M. and Krawinkler, H. (1993). "Effects of Soft Soil and Hysteresis Model on Seismic Demands", *Report 108, The John A. Blume Earthquake Engineering Center, Department of Civil and Environmental Engineering, Stanford University, Stanford, U.S.A.*
23. Riddell, R. and Newmark, N.M. (1979). "Statistical Analysis of the Response of Nonlinear Systems Subjected to Earthquakes", *Report UILU-ENG 79-2016, Department of Civil Engineering, University of Illinois at Urbana-Champaign, Urbana, U.S.A.*
24. Rosenblueth, E. and Herrera, I. (1964). "On a Kind of Hysteretic Damping", *Journal of the Engineering Mechanics Division, Proceedings of ASCE*, Vol. 90, No. EM4, pp. 37–48.
25. Ruiz-Garcia, J. and Miranda, E. (2003). "Inelastic Displacement Ratios for Evaluation of Existing Structures", *Earthquake Engineering & Structural Dynamics*, Vol. 32, No. 8, pp. 1237–1258.
26. Sadhu, A. (2007). "Ordered Peak Response under Multi-Component Ground Motion via Model Combination Rule and Its Correlation with Nonlinear Response", *M.Tech. Thesis, Indian Institute of Technology Kanpur, Kanpur.*
27. SEAOC (1995). "Vision 2000: A Framework for Performance-Based Earthquake Engineering, Vol. I", *Structural Engineers Association of California, Sacramento, U.S.A.*
28. Sen, N. and Gupta, V.K. (2018). "On Estimation of Seismic Damage from Ductility and Hysteretic Energy Demands in Equivalent Oscillators Using Linear Response", *Engineering Structures*, Vol. 172, pp. 663–686.
29. Shimazaki, K. and Sozen, M.A. (1984). "Seismic Drift of Reinforced Concrete Structures", *Technical Research Report, Hazama-Gumi Ltd., Tokyo, Japan* (in Japanese).
30. Veletsos, A.S. and Newmark, N.M. (1960). "Effect of Inelastic Behavior on the Response of Simple Systems to Earthquake Motions", *Proceedings of the Second World Conference on Earthquake Engineering, Tokyo-Kyoto, Japan*, Vol. II, pp. 895–912.
31. Veletsos, A.S., Newmark, N.M. and Chelapati, C.V. (1965). "Deformation Spectra for Elastic and Elastoplastic Systems Subjected to Ground Shock and Earthquake Motions", *Proceedings of the Third World Conference on Earthquake Engineering, Auckland-Wellington, New Zealand*, Vol. II, pp. 663–682.
32. Whittaker, A., Constantinou, M. and Tsopelas, P. (1998). "Displacement Estimation for Performance-Based Seismic Design", *Journal of Structural Engineering, ASCE*, Vol. 124, No. 8, pp. 905–912.